Carbohydrate Polymers 86 (2011) 469–476

Contents lists available at ScienceDirect

Carbohydrate Polymers

journal homepage: www.elsevier.com/locate/carbpol

Characterization of xanthan gum produced from sugar cane broth

Sandra Faria[a], Carmen Lúcia de Oliveira Petkowicz[b], Sérgio Antônio Lemos de Morais[c], Manuel Gonzalo Hernandez Terrones[c], Miriam Maria de Resende[a,*], Francisca Pessoa de França[d], Vicelma Luiz Cardoso[a]

[a] Faculty of Chemical Engineering, Federal University of Uberlândia, P.O. Box 593, 38400-902 Uberlândia, MG, Brazil
[b] Department of Biochemistry and Molecular Biology, Federal University of Paraná, Polytechnic Center, P.O. Box 19037, Curitiba, PR, Brazil
[c] Institute of Chemical, Federal University of Uberlândia, P.O. Box 593, 38400-902 Uberlândia, MG, Brazil
[d] Chemical Institute, Federal Universty of Rio de Janeiro, P.O. Box 378, 88030-400 Rio de Janeiro, RJ, Brazil

ARTICLE INFO

Article history:
Received 7 December 2010
Received in revised form 12 April 2011
Accepted 25 April 2011
Available online 5 May 2011

Keywords:
Sugarcane broth
Biopolymers
Xanthan gum
Rheological properties
Molecular characterization

ABSTRACT

Xanthan gum was produced by *Xanthomonas campestris pv. campestris* NRRL B-1459 using diluted sugar cane broth in experiments that lasted 24 h. The components used were in g/L: 27.0 sucrose; 2.0 Brewer's yeast; and 0.8 NH_4NO_3. The mixture was fermented at 750 rpm and 0.35 vvm. These conditions produced xanthan gum with the desired molecular weight and total sugar content, which were 4.2×10^6 Da and 85.3%, respectively. The sugar consisted of 43% glucose, 32% mannose and 24% glucuronic acid in a 1.79:1.33:1 ratio. The xanthan gum produced by this method was confirmed by comparing the infrared spectrum of commercial xanthan gum with the infrared spectrum of the xanthan gum produced using this method. The infrared spectra were very similar, which confirmed the identity the xanthan gum produced using our method. The xanthan gum was also evaluated using Proton Nuclear Magnetic Resonance (^{1}H NMR).

1. Introduction

Among the microbial gums, xanthan occupies a prominent place in the market by having rheological properties that are quite different and unusual, such as a high degree of pseudoplasticity, a high viscosity even at low concentrations, stability and compatibility with most metallic salts, excellent solubility and stability in acidic and alkaline solutions and resistance to degradation at elevated temperatures and various pH levels. The xanthan gum was liberated by FDA (Food and Drug Administration) in 1969, allowing its use in the in the production of foods (FAO/WHO, 1990). The gum exhibits many advantages as a thickener, stabilizer, gelling agent and suspending agent, as creams, artificial juices, sauces for salads, meat, chicken or fish, as well as for syrups and coverings for ice creams and desserts. It still presents compatibility with most of the colloids used in foods, including the starch, fact that turns its ideal for the preparation of breads and other products for breadmaking (Luvielmo & Scamparini, 2009; Nussinovitch, 1997). When used in low concentrations, it generates stability in the stockpiling, resistance capacity to the water and aesthetic appeal (Nussinovitch, 1997). Xanthan gum is also used in flocculation in food, petroleum (in process of perforations for oil recovery), pharmaceutical, cosmetics, paint, textile and agricultural products (in suspensions, as an agent for stabilizing herbicides, pesticides, fertilizers and fungicides) (Ashtaputre & Shah, 1995; García-Ochoa, Santos, Casas, & Gómez, 2000; Mulchandani, Luong, & Leduy, 1988).

The primary structure of xanthan was established in 1975 (Jansson, Kenne, & Lindberg, 1975). It consists of a pentasaccharide unit composed of glucose, mannose and glucuronic acid at a 2:2:1 ratio, as well as pyruvate and acetyl substituent groups. The main chain (backbone) of this gum is formed by units of β-D-glucose, which are linked at positions 1 and 4. The chemical structure of the polymer skeleton is therefore identical to that of cellulose (Jansson et al., 1975; Marzocca, Harding, Petroni, Cleary, & Ielpi, 1991; Morris, Brownsey, & Ridout, 1993; Rosalam & England, 2006).

The major producers of xanthan in the US are Merck, Kelco, and Pfizer. In France, the major producers of xanthan gum are Rhone Poulenc, Mero-Rousselot-Santia and Sanofi-Elf. In China, the major producer of xanthan gum is Saidy Chemical. The major producer of xanthan gum in Austria is Jungbunzlauer (García-Ochoa et al., 2000; Pradella, 2006). The market capitalization of xanthan gum is approximately US$270 million, and projections for 2015 exceed US$400 million (Pradella, 2006). For supply the various sectors of consumption were produced 86,000 tons/year of xanthan gum (Vorholter et al., 2008).

* Corresponding author. Tel.: +55 34 3239 4249; fax: +55 34 3239 4188.
E-mail address: mresende@feq.ufu.br (M.M. de Resende).

0144-8617/$ – see front matter © 2011 Elsevier Ltd. All rights reserved.
doi:10.1016/j.carbpol.2011.04.063

The carbon sources commonly used in the synthesis of xanthan gum are carbohydrates, such as starch, hydrolyzed starch, corn syrup, hydrolyzed rice, barley and corn flour, acid whey, sugarcane molasses, coconut juice, sugar cane, beet molasses, date juice palm, corn steep liquor, glucose and sucrose, etc., but glucose is still the best in terms of product yield, supply, and product quality (De Vuyst & Vermeire, 1994; El-Salam, Fadel, & Murad, 1994; García-Ochoa, Santos, & Alcon, 2004; Kalogiannis, Iakovidou, Liakopoulou-Kyriakides, Kyriakidis, & Skaracis, 2003; Kongruang, 2005; Rosalam & England, 2006; Salah, Chaari, Besbes, Blecker, & Attia, 2011). Brazil occupies a privileged position as a producer of sugarcane. Sugarcane juice is a noble raw material because it has an high concentration of sucrose, mineral salts and vitamins, which gives it an exceptional nutritional value. These aspects, among others, make it an excellent base for the production of xanthan gum. In this case, Brazil could stop importing xanthan gum and become a producer, with the advantage of operating plants at comparatively lower costs. This approach would put Brazil in a position to offer xanthan gum at market prices below those of the international market because the raw material requires minimal supplementation and processing expenses. The literature presents few information about the characterization of xanthan gum produced directly of sugar cane broth.

Based on the considerations mentioned above, the objective was to characterize xanthan gum biosynthesized from sugar cane broth, and analyze the chemical composition and quantify its monosaccharide, obtain information of rheological behavior to understand the mechanism of thermal decomposition and collect data from the infrared spectra and ^{1}H NMR.

2. Materials and methods

2.1. Raw material

The experiments were conducted using sugar cane broth as a source of sucrose. The cane used was courtesy of the owners of farms that are located in the municipality of Araporã – Brazil. The cane was collected and ground, and the filtered broth was stored at low temperature (-5 ± 1 °C) under aseptic conditions throughout the entire experiment.

2.2. Xanthan gum production

The inoculum was composed of 10% (v/v) from a medium grown under agitation (150 rpm) in a shaker at a temperature of 28 ± 1 °C for 16 h. The medium used for preparation of the inoculum in g/L: 20.0 sucrose, 3.0 yeast extract, 0.86 NH_4NO_3, 2.5 Na_2HPO_4 and 2.5 KH_2PO_4 (Alves, 1991; Lima, 1999; Serrano-Carreón, Corona, Sánchez, & Galindo, 1998). The average cellular concentration of inoculum was 0.29 ± 0.05 g/L.

The experiments were conducted using a Biostat B fermentor with a 6.0 L capacity that contained 4.0 L of medium.

The production medium used was optimized (Faria, Vieira, Resende, França, & Cardoso, 2009) and consisted of the following in g/L: 27.0 sucrose, 2.0 yeast extract, 0.8 NH_4NO_3, 2.5 Na_2HPO_4, 2.5 KH_2PO_4 and 0.5 antifoam. During the process, agitation and aeration were set to 750 rpm and 0.35 vvm, respectively. The temperature was 28 ± 1 °C, and the process time was 24 h.

All experiments were performed twice, and pH was maintained at 7.5 by adding 1N NaOH during the fermentation process. The sterilization of the carbon source and mineral solution was carried out separately under different conditions of pressure and temperature.

2.3. Recovery and purification of gum

The fermented medium was diluted with water at a ratio of 1:1 and processed in a centrifuge (Beckman Coulter Avanti J-25) with a relative centrifugal field of $18{,}900 \times g$ for 40 min to remove the cells. The supernatant was vacuum filtered through successive cellulose acetate membranes (Millipore) with porosities of 5, 3, 1.2 and 0.8 μm that were treated with KCl solution. The polymer was recovered by precipitation with ethanol. For 10 mL of centrifuged medium 3 mL of saturated solution of KCl and 30 mL of absolute ethanol were added to obtain xanthan gum (Ramírez, Fucikovsky, García-Jiménez, & Galindo, 1988). Report suggests washing the precipitate with ethanol solutions of increasing concentrations equal to 70%, 80%, 90% and absolute ethanol for about 10 min (Alves, 1991). The product was dried in Petri dishes covered with perforated plastic film in an oven at 30 ± 1 °C.

2.4. Evaluation of rheological behavior

The rheological characterization of aqueous solutions of the biopolymer was determined using a Brookfield viscometer LVDV-III Ultra. We used data about shear stress that was measured from strain rates according to the model of Ostwald de Waele or power-law (Chhabra & Richardson, 1999). We obtained K (consistency index) and n (behavior index) for xanthan solutions (0.75% (w/v) from Saporiti in Brazil) from the values of τ (shear tension) and γ (deformation rate) that were statistically evaluated using a nonlinear estimation. Thus, the apparent viscosity for a fluid power-law was determined from Eq. (1):

$$\mu_a = \frac{\tau}{\gamma} = K(\gamma)^{n-1} \tag{1}$$

2.5. Preparation of xanthan gum solutions for rheological analysis

After drying at 30 °C the gum was stored in a vacuum desiccator. In powder form, the gum looks similar to cornstarch. The procedure for hydration (0.75%, w/v) of the solutions was accomplished using magnetic stirring over a period of approximately 10 h (López, Vargas-García, Suarez-Estrella, & Moreno, 2004).

All solutions of the biopolymer were prepared by weight with moisture content approximately equal to 15% for commercial xanthan gum and the xanthan gum produced in this work.

2.6. Determination of intrinsic viscosity of xanthan gum samples

Polysaccharide solutions of 0.5, 0.25, 0.1, 0.05, 0.025 and 0.01 g/L were prepared in aqueous 0.1 M KCl. The original solution (0.5 g/L) was kept under agitation at 150 rpm and 25 °C for 18 h. For complete dissolution of the samples (commercial xanthan (CX) and xanthan gum produced under the conditions (Faria et al., 2009) (PX)), the solution was heated to 60 °C for 40 min before being used to make the other dilutions (Lima, 1999).

The relative, specific, reduced and intrinsic viscosities are given by Eqs. (2)–(5), respectively:

$$\eta_{\text{rel.}} = \frac{\eta}{\eta_0} \tag{2}$$

$$\eta_{\text{sp}} = \frac{\eta_{\text{solution}} - \eta_{\text{solvent}}}{\eta_{\text{solvent}}} = \eta_{\text{rel. solution}} - 1 \tag{3}$$

$$\eta_{\text{red.}} = \frac{\eta_{\text{sp}}}{C} \tag{4}$$

$$[\eta] = \lim_{C \to 0} \left(\frac{\eta_{\text{sp}}}{C} \right) \tag{5}$$

The intrinsic viscosity is obtained by graphically extrapolating the relationship between reduced viscosity and concentration. η

represents the effect of a single particle (without the influence of intermolecular interactions) on the viscosity of the solvent. Statistica 7.0 software was used to calculate the linear regressions and to obtain graphs of η_{sp}/C as a function of concentration (C).

2.7. Determination of total sugar content

The monosaccharide profile and determination of molecular weight of PX were performed at the Polytechnic Center of Federal University of Paraná by the Department of Biochemistry and Molecular Biology – Brazil.

The total sugar content was determined with phenol–sulfuric acid (Dubois, Gilles, Hamilton, Rebers, & Smith, 1956). The reading was made at a wavelength of 490 nm using a glucose solution as the standard at concentrations of 20–100 μg/mL. The measurements were repeated three times.

2.8. Determining the composition of neutral sugars

Samples of xanthan gum that weighed 2 mg were subjected to total acid hydrolysis. The hydrolysis was performed with 2 M trifluoroacetic acid (TFA) in a hermetically sealed tube at 100 °C for 5 h. After hydrolysis, excess acid was removed by evaporation (Biermann, 1989). The hydrolyzed material was washed twice with distilled water and evaporated to dryness.

Monosaccharides resulting from total acid hydrolysis were reduced with sodium borohydride ($NaBH_4$) at room temperature for 16 h in aqueous solution (Wolfrom & Thompson, 1963a). Hydride ions (H^-) supplied by the reducing agent ($NaBH_4$) reduce carbonyl groups of monosaccharides to form alditols. The residue was added to resin Lewatit S-100 (cation exchange resin in acid form) to decompose the excess reducing agent and remove the Na^+ cations.

The solution was filtered through cotton, and the filtrate was evaporated to dryness. Successive washings with 3 mL of methanol (3 times) removed the remaining boric acid. The resulting dry alditols were acetylated with pyridine (catalyst) and acetic anhydride (acetylating agent) (1:1, v/v) in tightly sealed hydrolysis tubes for 16 h at 25 °C (Wolfrom & Thompson, 1963b).

Crushed ice was then added to the system, and the resulting alditol acetates were extracted with 1 mL of chloroform. The residual pyridine was complexed with an aqueous solution of copper sulfate ($CuSO_4$) (5%). The pyridine–copper complex was separated from the chloroform phase and eliminated by successive washes with distilled water and $CuSO_4$.

The chloroform phase containing the alditol acetates was collected and dried. The sample was resolubilized in acetone for analysis by gas–liquid chromatography (GLC).

GLC analysis was carried out using a Hewlett Packard model 5890 A Series II gas chromatograph with flame ionization detector (FID) and injector with a temperature of 250 °C, capillary column DB-210 (30 m × 0.25 mm internal diameter) with film thickness of 0.25 μm at 220 °C and nitrogen as carrier gas with a flow rate of 2.0 mL/min.

2.9. Determination of sugar acids

The determination of uronic acids was performed using the method of Filisetti-Cozzi and Carpita (1991) with glucuronic acid as a standard solution with concentrations of 20–100 μg/mL and reading at 525 nm. The measurements were made three times.

2.10. Analysis by high-pressure steric exclusion chromatography and determination of molecular weight

The sample was solubilized in a solution of sodium nitrite ($NaNO_2$) 0.1 M containing sodium azide (NaN_3) at a 1–3 mg/mL concentration and filtered through an acetate cellulose (Millipore) membrane with a porosity of 0.2 μm.

The sample was injected into the high-pressure steric exclusion chromatograph (HPSEC) from Waters that is equipped with a Waters 2410 differential refractive index detector (RI) and a Multi-Angle Laser light scattering (MALLS) detector (Wyatt Technology Dawn DSP model) with 18 channels coupled in series. Four gel-permeation columns from Waters were used in series with exclusion limits of 7×10^6, 4×10^5, 8×10^4 and 5×10^3 g/mol. Analyses were performed at 25 °C using a 0.1 M solution of $NaNO_2$ containing 200 ppm NaN_3 as eluent with a flow rate of 0.6 mL/min in peristaltic pump (Waters 515).

The rate of change of the refractive index with concentration (dn/dc) was determined using five different concentrations. For this, a solution of 1 mg/mL in $NaNO_2$ 0.1 M containing 200 ppm NaN_3 was prepared, filtered through a 0.22 μm membrane and then diluted. The molecular mass was determined from the elution profile and the value of dn/dc with the calculations performed by the ASTRA software.

2.11. Thermal analysis (TGA/DTA)

Non-isothermal experiments were carried out by the Institute of Chemistry – Brazil, on a Shimadzu thermogravimetric (60H detector) module coupled to a thermal analyzer, using a heating rate of 20 °C/min under a dynamic atmosphere of nitrogen with a flow rate of approximately 30 mL/min to obtain TGA/DTA curves. The masses of samples required (CX and PX) were around 5.5 mg. The maximum temperature in the aluminum sample holder was 600 °C.

2.12. Spectroscopy of Fourier transform infrared (FTIR)

The infrared spectroscopic analysis was performed at the Facility of Chemical Engineering at Federal University of Uberlandia – Brazil. Samples of commercial xanthan (CX) and produced xanthan (PX) were analyzed on Bruker Equinox 55 equipment, operated in the spectral window from 400 to 4000 waves/cm with 32 scans/sample with a resolution of 4 waves/cm and scanning speed detector DTGS equal to 10 kHz. Three spectra were acquired sequentially for each sample. These spectra were processed and analyzed with the aid of OriginPro 7.5 software.

2.13. Determination by ^1H NMR

The ^1H NMR spectra of the produced xanthan gum were determined on a Bruker 250 MHz spectrometer at the Institute of Chemistry at the State University of Campinas, Brazil. Analyses were performed at 25 °C, 50 °C, 70 °C and 90 °C. The samples used by the Analytical Center contained about 20 mg of xanthan gum that was solubilized in 0.6 mL of deuterated water (D_2O).

3. Results and discussion

3.1. Determination of monosaccharide composition

The total sugar content found for the PX was 85.3%, and its monosaccharide composition was 43% glucose, 32% mannose, 24% glucuronic acid, which constitutes a ratio of 1.79:1.33:1. An correlation between the characteristics of microbial polysaccharides, focusing on structural, biosynthetic mechanisms, effects of genetic

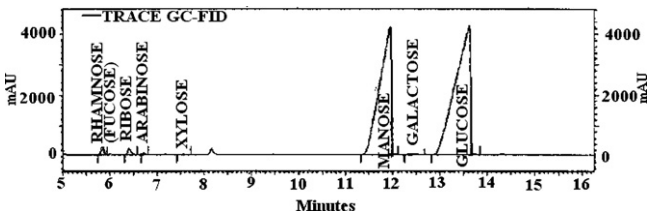

Fig. 1. Chromatogram of hydrolysis products of PX sample analyzed by gas–liquid chromatography in the form of alditol acetates.

engineering, physical properties associated with the chemical composition were showed by Sutherland (2001). Were found for *X. campestris* BD9A for glucose, mannose and glucuronic acid the ratio of 2.0:0.8:0.8, and showed to *X. campestris* (ratio of 2.0:1.8:1.0) values very close to those found in this work to *Xanthomonas campestris pv. campestris* NRRL B-1459 (Sutherland, 2001).

Even small variations in the composition of carbohydrates occur frequently depending on the strain employed. In many cases, the ratio of the monosaccharides is 1:1 (Silva et al., 2009). Other carbohydrates, such as rhamnose, arabinose, xylose and galactose were also detected at lower concentrations. The predominance of monomers of glucose and mannose and glucuronic acid in the hydrolyzate is in accordance with literature (Hamcerencu, Desbrieres, Popa, Khoukh, & Riess, 2007; Jansson et al., 1975; Marzocca et al., 1991; Morris et al., 1993; Salah et al., 2011; Silva et al., 2009). The concentration of acetate and pyruvate may vary depending on the conditions used in the fermentation process and post-fermentation because some properties of xanthan gum are directly related to the amounts of these substituents. Therefore, it is important to determine their concentrations.

The chromatogram shown in Fig. 1 represents the peaks of the hydrolysis products analyzed by gas liquid chromatography of produced xanthan samples.

3.1.1. Analysis by high pressure steric exclusion chromatography and molecular weight determination

The elution profile of the sample by HPSEC-MALLS/RI (Fig. 2) showed a unimodal mass distribution, which results from a polydispersity (M_W/M_N) equal to 1.014. This polydispersity value shows homogeneity in the material analyzed.

The weight-average molecular weight (M_W) obtained for xanthan, PX, was 4.2×10^6 Da. This value causes solutions of xanthan gum to be highly viscous with pseudoplastic character, which is discussed in later sections.

Batch fermentations performed in the range between 100 and 600 rpm and reported the influence of agitation in the chemical structure of xanthan gum and noted an increase in the level of pyruvate due to the increase in levels of agitation (Papagianni et al., 2001). Also, indicated an average molecular weight range typical of gum located between 2.0×10^6 and 5.0×10^7 Da (Papagianni et al., 2001). Molecular weight (M_W) determination of xanthan gum showed that it ranged from 0.8 to 1.4×10^6 Da obtained upon growth on a molasses concentration of 105 g/L (Kalogiannis et al., 2003).

3.2. Spectroscopic analysis (FT-IR)

The Fourier Transform-infrared spectrum (FT-IR) is a methodology to detect similarities or differences in chemical structures of compounds.

Samples of CX and PX were analyzed to identify the functional groups present in the structure of these biopolymers. The region studied included all the spectral bands located in the window between the wave numbers 400 and 4000 cm^{-1}.

Fig. 3 shows the infrared spectra of PX and CX. The most important bands recorded in the range of 4000–400 cm^{-1} were: (3200–3450 cm^{-1}: axial deformation of –OH; 2850–2950 cm^{-1}: axial deformation of C–H (may be due to absorption of symmetrical and asymmetrical stretching of CH_3 or even groups of CH_2) and CHO; 1710–1730 cm^{-1}: axial deformation of C=O ester, acid carboxylic, aldehydes and ketones; 1530–1650 cm^{-1}: axial deformation of C=O of enols (β-diketones); 1420–1430 cm^{-1}: deflection angle C–H; and 1050–1150 cm^{-1}: axial deformation of C–O).

Fig. 3 shows that the infrared spectrum of the (CX) is very similar to that obtained for the PX using the strain of *Xanthomonas campestris pv. campestris* NRRL B-1459. According to this result, we can infer that the isolated polysaccharide followed the same spectral behavior as the standard used because of similar methods employed by the manufacturer and the techniques used in this research.

Polysaccharide synthesized from *Pseudomonas oleovorans* NRRL B-14682 that was composed mainly of galactose and minor

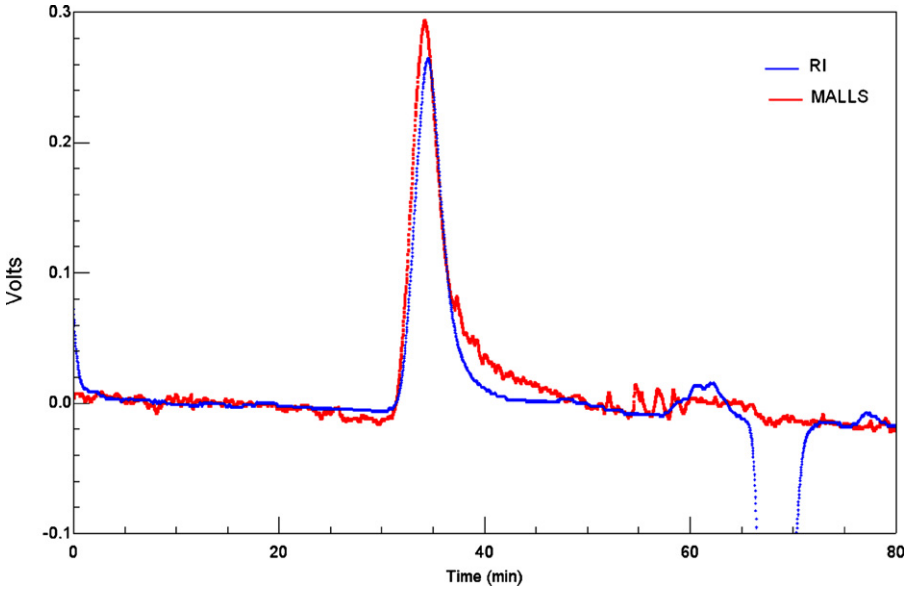

Fig. 2. HPSEC elution profile with detectors of refractive index (RI) and light scattering (MALLS – showed the angle of 90°).

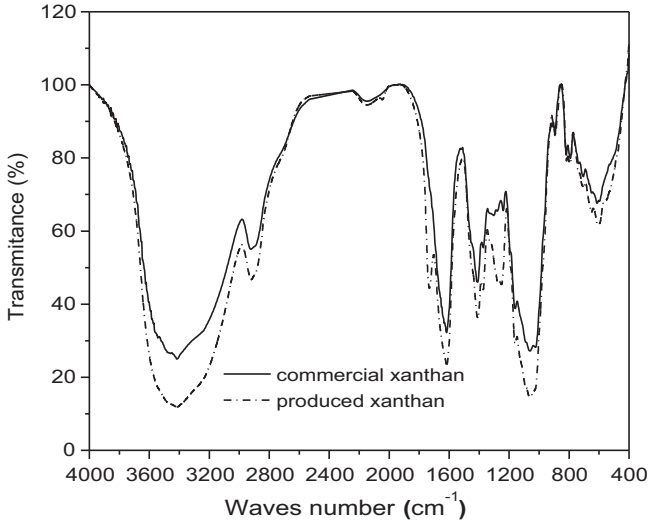

Fig. 3. FT-IR spectrum of xanthan samples in KBr pellets for CX and PX.

amounts of mannose, glucose and rhamnose using glycerol as carbon source (Freitas et al., 2009). Comparing the FT-IR spectrum of other commercial gums, guar and xanthan, they concluded that the bands around 3400 cm^{-1}, 2939 cm^{-1} and 990–1200 cm^{-1} that are common to all polysaccharides represent O–H bonds, C–H bonds of CH_2 groups and saccharides, respectively. The correspondence between bands led them to assert a strong similarity between exopolysaccharide (EPS) and (PX) due to the acid groups present. However, infrared spectroscopy alone is not conclusive in identifying the structure of polysaccharides of interest; therefore, we recommend the use of complementary techniques, such as proton and carbon Nuclear Magnetic Resonance spectroscopy.

3.3. Rheological behavior of xanthan solutions with a concentration of 0.75% (w/v)

An important feature associated with biopolymers is their ability to cause thickening at a certain concentration, usually less than 1% (w/v), promoting high viscosities at known strain rates.

Fig. 4a and b represents the rheograms generated from OriginPro 7.5 software using measurements of strain rates to shear stress applied to a 0.75% (w/v) solution of xanthan gum.

For CX, K and n are assumed to be equal to 6.442 [Pa s^n] and 0.136 (Fig. 4a), respectively. The xanthan gum produced in this study produced K and n values equal to 13.257 [Pa s^n] and 0.226, respectively (Fig. 4b). These results are significant because, in the case of pseudoplastic fluids, the shear stress is a nonlinear function of strain rate and also depends on temperature, pressure, molecular weight and molecular morphology. However, caution is required when comparing these parameters because they represent the rheological parameters of gum from different fermentation processes.

3.4. Determination of the intrinsic viscosity of xanthan gum

The intrinsic viscosities of CX and PX at the optimal point were 3967.8 mL/g and 2862.6 mL/g, respectively (Fig. 5). This difference led to consolidated discussions about the size, shape and molecular weight of the structure, which were relevant to the characterization process. Viscometric measurements in dilute solutions may show peculiarities at the molecular level. Viscometric measurements are a useful tool in determining the chemical composition of EPSs synthesized by fermentation (Lima, 1999).

Values of intrinsic viscosity of samples of xanthans that were polymerized in a synthetic medium from three strains of *Xanthomonas* (Lima, 1999) were on the same order of magnitude as those obtained in this study. In this sequence for *Xanthomonas campestris pv. campestris* NRRL B-1459, LFR-3 (isolated from cabbage – *Brassica oleracea* var. *capitata*), and LFR-4 (isolated from radish – *Raphnus sativus* L.), the intrinsic viscosities were 3500.71, 1125.3 and 2210.3 mL/g, respectively (Lima, 1999).

There are many ways to explain the variation reported in the literature for the intrinsic viscosity, such as different strains and recovery procedures and different types of pre-treatment that are used on solutions of xanthan before viscosity determination, such as filtration, heating, and centrifugation (Galindo, Salcedo, Flores, & Ramirez, 1993).

The effects of three salts (NaCl, KCl and $CaCl_2$) were investigated on the viscoelastic properties of xanthan, locust bean gum (LBG) and their blends (Higiro, Herald, Alavi, & Bean, 2007). In the absence of salts, xanthan 60%–LBG 40% showed the highest intrinsic viscosity due to the strong attraction between molecules. Any of the added salts, regardless of the solutions analyzed, sharply reduced the intrinsic viscosity with pronounced effects from divalent ions compared to monovalent ions.

3.5. Thermal evaluation of commercial xanthan and produced xanthan gum (TGA–DTA)

TGA–DTA curves properly interpreted (Figs. 6 and 7) illustrate the mechanism of thermal decomposition to two samples of

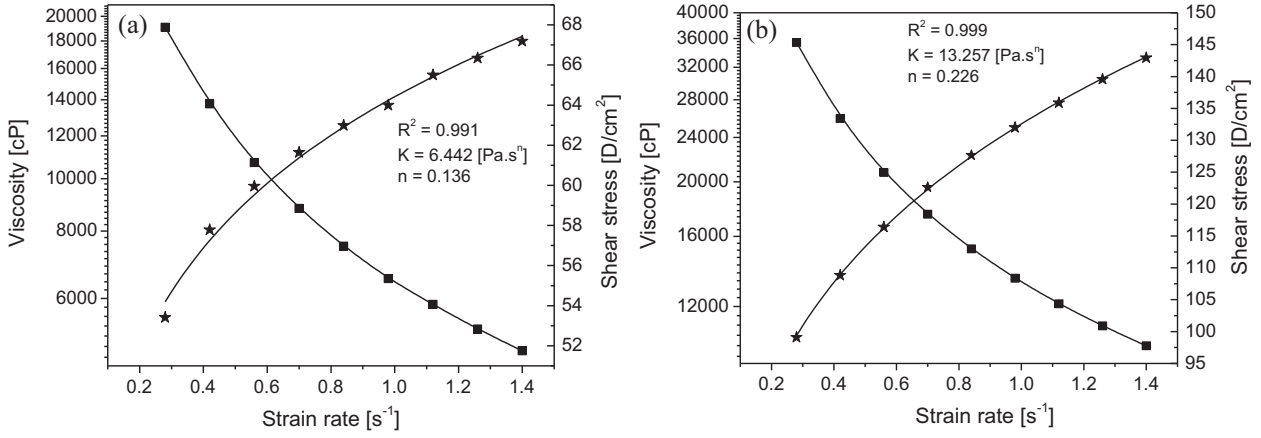

Fig. 4. Viscosity curves. (a) Shear stress as a function of strain rate for CX (0.75% solution) and (b) shear stress as a function of strain rate considering the xanthan in the conditions (0.75% solution).

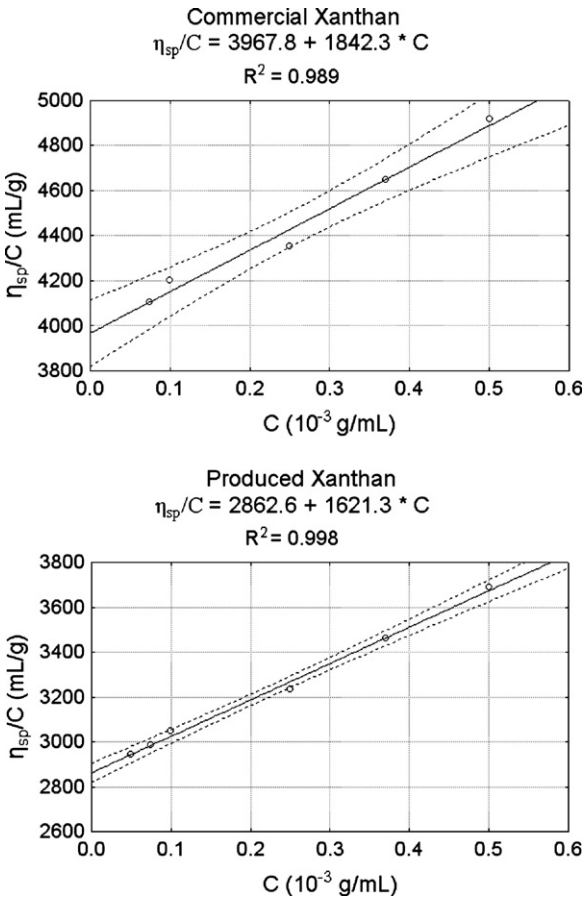

Fig. 5. Linear regression of $(\eta_{sp}/C) \times C$ to obtain the intrinsic viscosity of xanthan gum: CX and PX.

xanthan gum. The first mass loss (30–140 °C) associated with the endothermic peak is attributed to dehydration and corresponds to approximately 15% in both situations. Water absorption by xanthan is due to the presence of polar groups in its structure, especially the –OH grouping. Analysis of the TGA curves and its derivative (dTGA) showed that the maximum decomposition rate for the first thermal degradation occurs at a temperature of 58 °C and corresponds to the inflection point of the derivative. The second degradation process (220–320 °C) is accompanied by a weight loss exceeding 40%. Therefore, caution is necessary in the assessment of this thermal event for both the CX

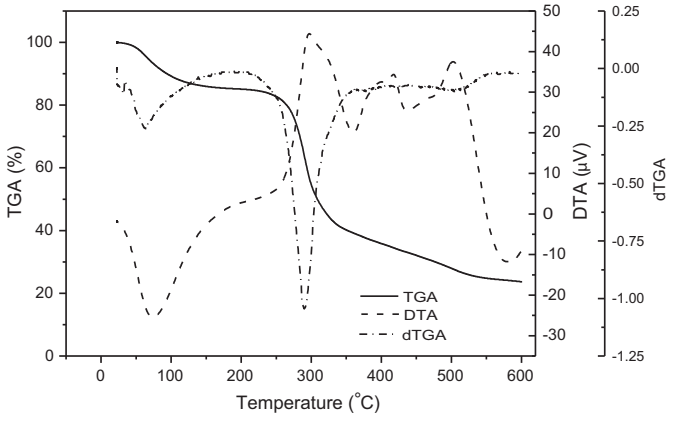

Fig. 6. Simultaneous TGA–DTA curves for (CX); heating rate equal to 20 °C/min and a nitrogen atmosphere with a flow rate of 30 mL/min.

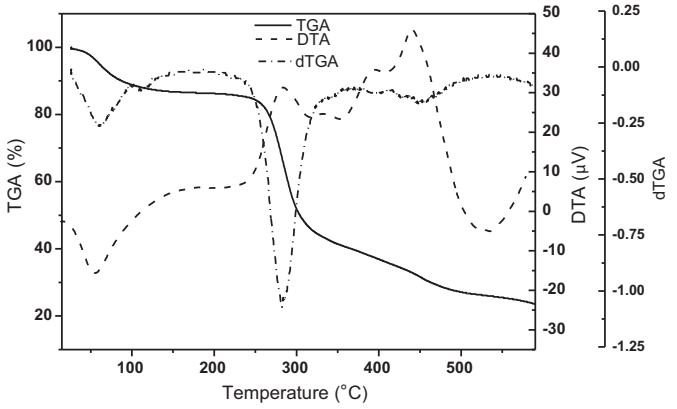

Fig. 7. Simultaneous TGA–DTA curves for PX; heating rate equal to 20 °C/min and a nitrogen atmosphere with a flow rate of 30 mL/min.

and PX. The temperatures obtained at the second stage and the maximum rate of decomposition was slightly different but that does not prevent the comparison between samples. We obtained 294 °C and 283 °C for CX and PX, respectively, which means that they have similar thermal stability. Based on the DTA curve, the thermograms also showed the predominance of exothermic processes in the second degradation and the subsequent secondary events.

TG data for different polysaccharides, including xanthan gum, were reported as stages of decomposition (Zohuriaan & Shokrolahi, 2004). They obtained a DTG maximum of 74.6 °C for xanthan gum in a single stage of decomposition with a temperature range of 30–91 °C. With two stages of decomposition with a temperature range of 251.5–330.3 °C, they obtained a DTG maximum of 290.8 °C. Thus, despite the small variations found for the bands associated with the thermal degradation of xanthan gum, it is known that several factors contribute, either separately or simultaneously, which affects the shape of the TGA–DTA curves. By comparing the thermal analysis of samples of xanthan to the literature, we found the need for additional research to elucidate the thermal behavior of gum, whether pure or associated (blends).

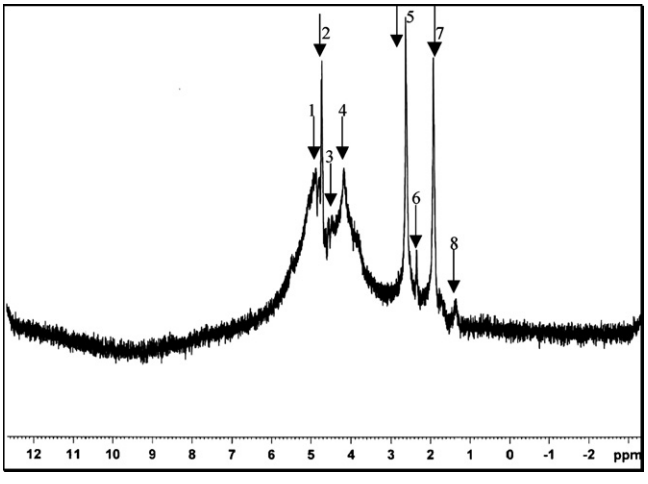

Fig. 8. Proton nuclear magnetic resonance (^{1}H-NMR) spectrum of PX in deuterated water (D_2O) at 70 °C. The α-anomeric protons in hexose or pentose (4.9 ppm) (2, 3), the β protons of hexose or pentose (4.6, 4.7 ppm), protons of carbons connected to oxygen (4.3 ppm) (5, 6, 7), proton of uronic and glucuronic acid (1.8, 2.3, 2.5 ppm) and the H6 proton of rhamnose (1.3 ppm). (7, 8) – may represent protons belonging to the acetyl group (1.3, 1.8 ppm).

3.6. Spectroscopic characterization by proton nuclear magnetic resonance

Xanthan gum has a rigid molecular conformation, which leads to strong dipole interactions between the nucleus of hydrogen and the nucleus of carbon. These dipole interactions result in an enlargement of the resonance line (Rinaudo, Milas, & Lambert, 1983). Thus, the signals are not detected in routine Proton Nuclear Magnetic Resonance (^{1}H NMR) (Lima, 1999).

At first, the ^{1}H NMR spectra obtained for the PX were performed at four temperatures (25 °C, 50 °C, 70 °C and 90 °C) to verify the experimental situation in which the signals can be better interpreted. In general, sodium acetate is used as a standard in low concentrations ($\cong 10^{-3}$ M) to quantify the levels of pyruvate and acetyl groups (Lima, 1999).

As shown in Fig. 8, the temperature that allowed the clearest identification of the signals was 70 °C. The collection of spectra performed in the absence of standard (sodium acetate) disabled the integration of signals related to pyruvate and acetyl groups. The amounts of pyruvate and acetyl groups depend on the bacterial strain and conditions of the fermentation process, such as fermentation time, carbon source and the availability of oxygen, nitrogen and other nutrients involved in the biosynthesis (Sandford et al., 1977). The variation of these groups changes the rheological properties of xanthan (Holzwarth & Ogletree, 1979).

Comparison of ^{1}H NMR spectra of exopolysaccharides from strains of *Xanthomonas oryzae pv. oryzae*, BXO1 and BXO8 and showed the presence of the α-anomeric proton of hexoses or pentoses at 5.1 and 5.2 ppm, protons of β carbons of hexoses or pentoses at 4.8 and 4.9 ppm, the hydrogen near the –OH group at 4.0 ppm and uronic acid of hexose or pentose located at 2.3 ppm. Structural variations were confirmed according to the distribution of carbohydrates to BXO1 and BXO8 (Singh et al., 2006).

4. Conclusions

The results showed that:

- The chemical characterization of exopolysaccharides showed the following relevant carbohydrates: glucose, mannose and glucuronic acid in a ratio of 1.79:1.33:1.
- The weight-average molecular weight (M_W) found for PX was 4.172×10^6 Da, which was provided by a polydispersity (M_W/M_N) equal to 1.014.
- The FT-IR spectrum of the PX followed the same pattern of emission bands of the CX.
- The ^{1}H NMR spectrum showed chemical shifts for α-anomeric protons of hexose or pentose, protons of β-carbon of hexose or pentose, protons of carbons connected to oxygen, proton H6 of rhamnose and protons of uronic and glucuronic acids.
- Thermal analysis showed that maximum degradation rates occurred at 294 °C for commercial xanthan gum and 283 °C for the xanthan gum biosynthesized in this study.

Acknowledgments

The authors wish to thank the CNPq, CAPES and FAPEMIG – Brazil for financial support.

References

Alves, R. S. A. (1991). *Efeito de alguns nutrientes na formação de goma xantana por Xanthomonas campestris pv LMI-3*. Materials and methods chapter. MS dissertation. BR: Chemical School, Federal University of Rio de Janeiro, 126 pp.

Ashtaputre, A. A., & Shah, A. K. (1995). Studies on a viscous, gel-forming exopolysaccharide from *Sphingomonas paucimobilis* GS1. *Applied and Environmental Microbiology*, *61*, 1159–1162.

Biermann, C. J. (1989). Hydrolysis and other cleavage of glycosidic linkages. In C. J. Biermann, & G. D. Mcginnis (Eds.), *Analysis of carbohydrates by GLC and MS* (pp. 27–41). Florida: CRC Press, 292 pp.

Chhabra, R. P., & Richardson, J. F. (1999). *Non-Newtonian flow in the process industries: Fundamentals and engineering applications. Non-Newtonian fluid behaviour and rheometry for Non-Newtonian fluids chapters*. Great Britain: Butterworth Heinemann., pp. 38–71, 421 pp.

De Vuyst, L., & Vermeire, A. (1994). Use of industrial medium components for xanthan production by *Xanthomonas campestris*. *Applied Microbiology and Biotechnology*, *42*, 187–191.

Dubois, M. A., Gilles, K. A., Hamilton, J. K., Rebers, P. A., & Smith, F. (1956). Colorimetric method for determination of sugars and related substances. *Analytical Chemistry*, *28*, 350–356.

El-Salam, M. H. A., Fadel, M. A., & Murad, H. A. (1994). Bioconversion of sugarcane molasses into xanthan gum. *Journal of Biotechnology*, *33*, 103–106.

FAO/WHO (Food and Agriculture Organization of the United Nations). (1990). *Production yearbook 1989*. Roma, Codebook, ECON-109 (1990).

Faria, S., Vieira, P. A., Resende, M. M., França, F. P., & Cardoso, V. L. (2009). A comparison between shaker and bioreactor performance based on the kinetic parameters of xanthan gum production. *Applied Biochemistry and Biotechnology*, *156*, 45–58.

Filisetti-Cozzi, T. M. C. C., & Carpita, N. C. (1991). Measurement of uronic acids without interference from neutral sugars. *Analytical Biochemistry*, *197*, 157–162.

Freitas, F., Alves, V. D., Pais, J., Costa, N., Oliveira, C., Mafra, L., et al. (2009). Characterization of an extracellular polysaccharide produced by a *Pseudomonas* strain grows on glycerol. *Bioresource Technology*, *100*, 859–865.

Galindo, E., Salcedo, G., Flores, C., & Ramirez, M. E. (1993). Improved shake-flask test for the screening of xanthan-producing microorganisms. *World Journal of Microbiology and Biotechnology*, *9*, 122–124.

García-Ochoa, F., Santos, V. E., & Alcon, A. (2004). Chemical structured kinetic model for xanthan production. *Enzyme and Microbial Technology*, *35*, 284–292.

García-Ochoa, F., Santos, V. E., Casas, J. A., & Gómez, E. (2000). Xanthan gum: production, recovery, and properties. *Biotechnology Advances*, *18*, 549–579.

Hamcerencu, M., Desbrieres, J., Popa, M., Khoukh, A., & Riess, G. (2007). New unsaturated derivatives of xanthan gum: Synthesis and characterization. *Polymer*, *48*, 1921–1929.

Higiro, J., Herald, T. J., Alavi, S., & Bean, S. (2007). Rheological study of xanthan and locust bean gum interaction in dilute solution: Effect of salt. *Food Research International*, *40*, 435–447.

Holzwarth, G., & Ogletree, J. (1979). Pyruvate-free xanthan. *Carbohydrate Research*, *76*, 277–280.

Jansson, P. E., Kenne, L., & Lindberg, B. (1975). Structure of the extracellular polysaccharide from *Xanthomonas campestris*. *Carbohydrate Research*, *45*, 275–282.

Kalogiannis, S., Iakovidou, G., Liakopoulou-Kyriakides, M., Kyriakidis, D. A., & Skaracis, G. N. (2003). Optimization of xanthan gum production by *Xanthomonas campestris* grown in molasses. *Process Biochemistry*, *39*, 249–256.

Kongruang, S. (2005). Growth kinetics of xanthan production from uneconomical agricultural products with *Xanthomonas campestris* TISTR 1100. *The Journal of Applied Science*, *4*(2), 78–88.

Lima, M. A. G. A. (1999). Obtenção e Caracterização de Xantanas Produzidas por Diferentes Linhagens de *Xanthomonas campestris pv. campestris*. Material and Methods chapter. Doctorate thesis. BR: Chemical School, Federal University of Rio de Janeiro.

López, M. J., Vargas-García, M. C., Suarez-Estrella, F., & Moreno, J. (2004). Properties of xanthan obtained from agricultural wastes acid hydrolysates. *Journal of Food Engineering*, *63*, 111–115.

Luvielmo, M. M., & Scamparini, A. R. P. (2009). Goma xantana: produção, recuperação, propriedades e aplicação. *Estudos tecnológicos*, *5*, 50–67.

Marzocca, M. P., Harding, N. E., Petroni, E. A., Cleary, J. M., & Ielpi, L. (1991). Location and cloning of the ketal pyruvate transferase gene of *Xanthomonas campestris*. *Journal of Bacteriology*, *173*, 7519–7524.

Morris, V. J., Brownsey, G. J., & Ridout, M. J. (1993). Acetan and related polysaccharides. *Polymer News*, *18*, 294–300.

Mulchandani, A., Luong, J. H. T., & Leduy, A. (1988). Batch kinetics of microbial polysaccharide biosynthesis. *Biotechnology and Bioengineering*, *32*, 639–646.

Nussinovitch, A. (1997). Hydrocolloid application – Gum technology in the food and other industries, Londres. *Blackie Academic e Professional*, 155–169, 354 p.

Papagianni, M., Psomas, S. K., Batsilas, L., Paras, S. V., Kyriakidis, D. A., & Liakopoulou-Kyriakides, M. (2001). Xanthan production by *Xanthomonas campestris* in batch cultures. *Process Biochemistry*, *37*, 73–80.

Pradella, J. G. C. (2006). *Biopolímeros e Intermediários Químicos, Relatório Técnico nº 84 396-205, Centro de Gestão e Estudos Estratégicos*. São Paulo: Laboratório de Biotecnologia Industrial – LBI/CTPP., 119 pp.

Ramírez, M. E., Fucikovsky, L., García-Jiménez, F., Quinteiro, & Galindo, E. (1988). Xanthan gum production by altered pathogenicity variants of *Xanthomonas campestris*. *Applied Microbiology and Biotechnology*, *29*, 5–10.

Rinaudo, M., Milas, M., & Lambert, F. (1983). ^{1}H and ^{13}C NMR investigation of xanthan gum. *Macromolecules*, *16*, 816–819.

Rosalam, S., & England, R. (2006). Review of xanthan gum production from unmodified starches by *Xanthomonas campestris* sp. *Enzyme and Microbial Technology*, *39*, 197–207.

Salah, R. B., Chaari, K., Besbes, S., Blecker, C., & Attia, H. (2011). Production of xanthan gum from *Xanthomonas campestris* NRRL B-1459 by fermentation of date juice palm by-products (*Phoenix dactylifera* L.). *Journal of Food Process Engineering*, *34*, 457–474.

Sandford, P. A., Pittsley, J. E., Knutson, C. A., Watson, P. R., Cadmus, M. C., & Jeanes, A. (1977). Variation in *Xanthomonas campestris* NRRL B-1459. Characterization of xanthan products of differing pyruvic acid content. *Extracellular Microbial Polysaccharides*, *45*, 192–209.

Serrano-Carreón, L., Corona, R. M., Sánchez, A., & Galindo, E. (1998). Prediction of xanthan fermentation development by a model linking kinetics, power drawn and mixing. *Process Biochemistry*, *33*, 133–146.

Silva, M. F., Fornari, R. C. G., Mazutti, M. A., Oliveira, D., Padilha, F. F., Cichoski, A. J., et al. (2009). Production and characterization of xantham gum by *Xanthomonas campestris* using cheese whey as sole carbon source. *Journal of Food Engineering*, *90*, 119–123.

Singh, V. B., Kumar, A., Kirubakaran, S. I., Ayyadurai, N., Kumar, R. S., & Sakthivel, N. (2006). Comparison of exopolysaccharides produced by *Xanthomonas oryzae pv. oryzae* strains, BXO1 and BXO8 that show varying degrees of virulence in rice (*Oryza sativa* L.). *Journal of Phytopathology*, *154*, 410–413.

Sutherland, I. W. (2001). Microbial polysaccharides from Gram-negative bacteria. Institute of Cell and Molecular Biology, University of Edinburgh, Mayfield Road, Edinburgh EH9 3JH, UK. *International Dairy Journal*, *11*, 663–674.

Vorholter, F.-J., Schneiker, S., Goesmann, A., Krause, L., Bekel, T., Kaiser, O., et al. (2008). The genome of *Xanthomonas campestris pv. campestris* B100 and its use for the reconstruction of metabolic pathways involved in xanthan biosynthesis. *Journal of Biotechnology*, *134*, 33–45.

Wolfrom, M. L., & Thompson, A. (1963a). Acetylation. *Methods in Carbohydrate Chemistry*, *2*, 211–215.

Wolfrom, M. L., & Thompson, A. (1963b). Reduction with sodium borohydride. *Methods in Carbohydrate Chemistry*, *2*, 65–67.

Zohuriaan, M. J., & Shokrolahi, F. (2004). Thermal studies on natural and modified gums. *Polymer Testing*, *23*, 575–579.